Birefringence of Plastically Deforming Polymer Solid in Loading and Unloading Processes Under Variable Stress Rates

INTRODUCTION

A theoretical birefringence relation for a plastically deforming polymer solid during loading process has been deduced by starting from the optical theory of deformable dielectrics.[1] From the experiments in the proportional loading[1] and in the creep tests[2] by using the cellulose nitrate at 65°C for the loading process, it was clarified that the deduced birefringence relation of the first-order approximation in the loading process gave good agreement with the experimental results independent of the value of constant stress rate and of the value of creep stress or the hydrostatic stress as shown in the previous notes,[1,2] respectively.

In this note, as a continuation of the loading process,[1] a birefringence relation in the unloading process is deduced by using the same postulates as in the loading process. In the real process of plastic deformation, the stress rate is not always constant throughout the whole process. For the purpose of examining whether the birefringence relations for the loading and unloading processes established under the constant stress rates are applicable with sufficient accuracy even for variable stress rates, the experiments are performed using the same cellulose nitrate as in the previous notes[1,2] under some variable stress rates which vary with time for the loading and unloading processes. As a result, the relations established under the constant stress rates for the loading and unloading processes give good agreement with the actual observations in each process under the variable stress rates.

BASIC RELATIONS OF BIREFRINGENCE

Experimental stress–strain relations during the loading and unloading processes under constant stress rates for plastically deforming cellulose nitrate are shown in Figure 1, where $\Delta\sigma$ and ΔG denote the difference of principal stresses and the difference of principal strains in the Green strain system[3] as shown in the previous notes,[1,2] and the point 0* in Figure 1 is the final point of the loading process. The loading process in Figure 1 corresponds to the proportional tests $\Delta\dot{\sigma} = 0.25$ and 2.0 MPa/min at 55°C, and the stress level in the unloading process of Figure 1 decreases with time at the same rate as in the loading process. In Figure 1, the unloading coordinate system whose axes have opposite directions to those of the preceding loading coordinate system is considered a new loading beginning at the point 0* of Figure 1. The physical quantities corresponding to the unloading process are labelled by superimposed bars. In the plastically deforming polymer, the strain tensor in the unloading process may be considered to consist of three parts, namely an elastic strain tensor $\overline{\mathbf{E}}_e$ ($\Delta\overline{G}_e$ in Fig. 1), a viscous recovery strain tensor $\overline{\mathbf{E}}_r$ ($\Delta\overline{G}_r$ in Fig. 1), and a viscous additional strain tensor $\overline{\mathbf{E}}_a$ ($\Delta\overline{G}_a$ in Fig. 1). The viscous additional part $\overline{\mathbf{E}}_a$ continues to appear in the early stage of the unloading process for the operating load even in the unloading process. The elastic and the inelastic strain tensors in the unloading process are regarded as $\overline{\mathbf{E}}_e$ and $\overline{\mathbf{E}}_i = \overline{\mathbf{E}}_r - \overline{\mathbf{E}}_a$.

The birefringent properties of a plastically deforming polymer depend upon the index tensor η in the dielectric field,[1,4,5] and the index tensor η in the loading process was proposed as[1,2]

$$\eta = \mathbf{F}(\mathbf{E}_e, \mathbf{E}_i), \tag{1}$$

where $\mathbf{E}_e$ and $\mathbf{E}_i$ are elastic and inelastic strain tensors in the loading process. The isochromatic fringe order per unit thickness N of photomechanics in the loading process for the first-order approximation was given by[1,2]

$$N = C_1(\Delta\sigma) + C_2(\Delta G_i) \tag{2}$$

Journal of Applied Polymer Science, Vol. 32, 5675–5684 (1986)
 CCC 0021-8995/86/065675-10$04.00

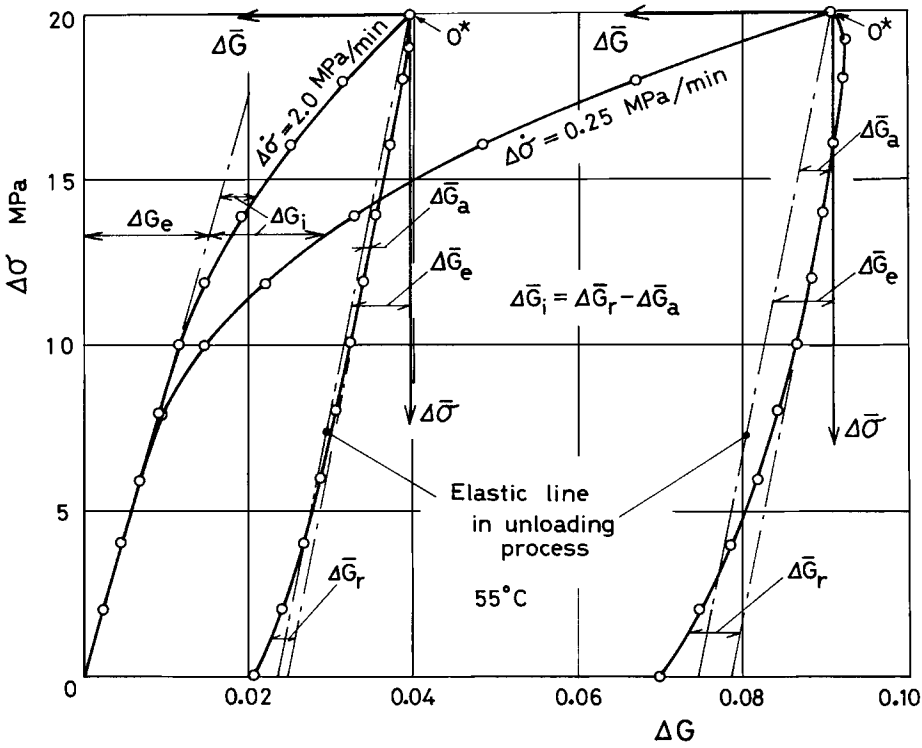

Fig. 1. Relations between $\Delta\sigma$ and ΔG for $\Delta\dot{\sigma}$ = 0.25 and 2.0 MPa/min.

where C_1 and C_2 are optical constants describing the loading process, $\Delta\sigma = \sigma_1 - \sigma_2$ is the difference of principal stresses, and $\Delta G_i = G_{i1} - G_{i2}$ is the difference of principal inelastic strains.[1,2]

The unloading process is considered as a new loading process beginning at the point 0* in Figure 1. By using the same postulates as in the loading process,[1] the index tensor $\bar{\eta}$ in the unloading process may be proposed as

$$\bar{\eta} = \bar{\mathbf{F}}(\bar{\mathbf{E}}_e, \bar{\mathbf{E}}_i) \tag{3}$$

where $\bar{\mathbf{F}}$ is polynomial isotropic function of two symmetric tensors.[6] The isochromatic fringe order per unit thickness $\bar{N}$ in the unloading process for the first-order approximation is also expressed by using the same procedures as in Eq. (2) describing the unloading process as follows

$$\bar{N} = \bar{C}_1(\Delta\bar{\sigma}) + \bar{C}_2(\Delta\bar{G}_i) \tag{4}$$

where $\bar{C}_1$ and $\bar{C}_2$ are optical constants describing the unloading process, $\Delta\bar{\sigma} = \bar{\sigma}_1 - \bar{\sigma}_2$ and $\Delta\bar{G}_i = \bar{G}_{i1} - \bar{G}_{i2}$. By introducing the fringe order N^* and the stress $\Delta\sigma^*$ at the final point 0* of the loading process in Figure 1, the fringe order and the stress during the unloading process can be expressed as

$$N = N^* - \bar{N} \quad \text{and} \quad \Delta\sigma = \Delta\sigma^* - \Delta\bar{\sigma} \tag{5}$$

VARIATIONS OF STRESS WITH RESPECT TO TIME

Variations of stress with respect to time may be expressed as the combinations of sinusoidal elements as an example. The four conditions shown in Table I are examined in the loading and unloading process by using three specimens for each case. The symbol t^* in Table I denotes

TABLE I
Relations Between Stress and Time in the Loading and Unloading Processes

	Condition	(a) $\Delta\sigma$ MPa	(b) $\Delta\sigma$ MPa
1	Loading	$17.16 \sin \frac{\pi t}{30}$	$17.16 \sin \frac{\pi t}{120}$
	Unloading	$17.16 \sin \frac{\pi(2t^* - t)}{30}$	$17.16 \sin \frac{\pi(2t^* - t)}{120}$
2	Loading	$2.288t - 17.16 \sin \frac{\pi t}{30}$	$0.572t - 17.16 \sin \frac{\pi t}{120}$
	Unloading	$2.288(2t^* - t) - 17.16 \sin \frac{\pi(2t^* - t)}{30}$	$0.572(2t^* - t) - 17.16 \sin \frac{\pi(2t^* - t)}{120}$
3	Loading	$1.144t - 2 \sin \frac{2\pi t}{15}$	$0.286t - 2 \sin \frac{\pi t}{30}$
	Unloading	$1.144(2t^* - t) - 2 \sin \frac{2\pi(2t^* - t)}{15}$	$0.286(2t^* - t) - 2 \sin \frac{\pi(2t^* - t)}{30}$
4	Loading	$1.144t + 2 \sin \frac{2\pi t}{15}$	$0.286t + 2 \sin \frac{\pi t}{30}$
	Unloading	$1.144(2t^* - t) + 2 \sin \frac{2\pi(2t^* - t)}{15}$	$0.286(2t^* - t) + 2 \sin \frac{\pi(2t^* - t)}{30}$

the time at the final point 0* of the loading process or at the beginning of the unloading process. The stress rate for the case (a) in Table I is larger than that for the case (b). The stress in the unloading process varies with the symmetrical mode to the case of loading process. Figure 2 shows the relations between $\Delta\sigma$ and time under the conditions 1(a), 1(b), to 4(a), 4(b) shown in Table I.

EXPERIMENTS

Tests were performed with the uniaxial cellulose nitrate specimens of 6 mm thick at 55°C in the uniaxial stress state: $\sigma_i = \Delta\sigma$, $\sigma_2 = \sigma_3 = 0$ as same as in the previous note.[1] On the surface of the specimen, a square gauge mark was incised in the region of uniform stress. The experimental apparatus consists of three major systems, namely, an oil vessel with heater, a loading system, and instruments to record the load and deformation. The detailed descriptions of the apparatus and the experimental procedure are shown in Ref. 7. Each load was applied so as to obtain variable stress rates as shown in Table I or Figure 2 at 55°C. Axial elongation and cross contraction over the distance between the gauge marks were measured by the same procedure as in the previous notes,[1,2] and the difference between the principal strains $\Delta G = (G_1 - G_2)$ was calculated in Green's strain system[1-3] $G_j = e_j + (e_j)^2/2$, where e_j ($j = 1, 2$) is the conventional engineering strain. The fringe order was measured by Tardy's method.[8,9]

Figure 3 shows the relations between $\Delta\sigma$ and the fringe order per unit thickness N at 55°C for the two values of constant stress rates corresponding to Figure 1, which were investigated for the sake of determining the optical constants involved in Eqs. (2) and (4). Each symbol in Figure 3 is plotted using the average value of the three test results. The values of optical constants in the loading process and in the unloading process at 55°C are $C_1 = 0.022\ \mathrm{MPa^{-1}mm^{-1}}$, $C_2 = 1.5\ \mathrm{mm^{-1}}$ and $\bar{C}_1 = 0.018\ \mathrm{MPa^{-1}mm^{-1}}$, $\bar{C}_2 = 4.2\ \mathrm{mm^{-1}}$, respectively. The broken curves in Figure 3 are calculated from Eq. (2) using the constants C_1, C_2, and ΔG_i as shown in Figure 1 for the loading process and from Eq. (4) using the constants $\bar{C}_1$, $\bar{C}_2$, and $\Delta\bar{G}_i$ as shown in the unloading process of Figure 1.

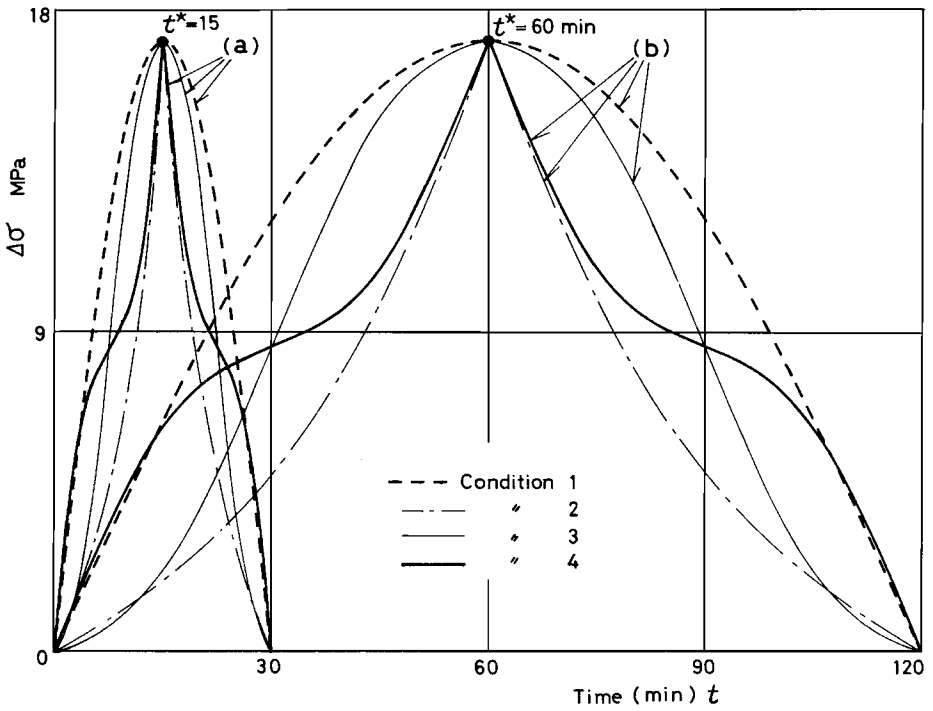

Fig. 2. Relations between $\Delta\sigma$ and time under the four conditions of Table I.

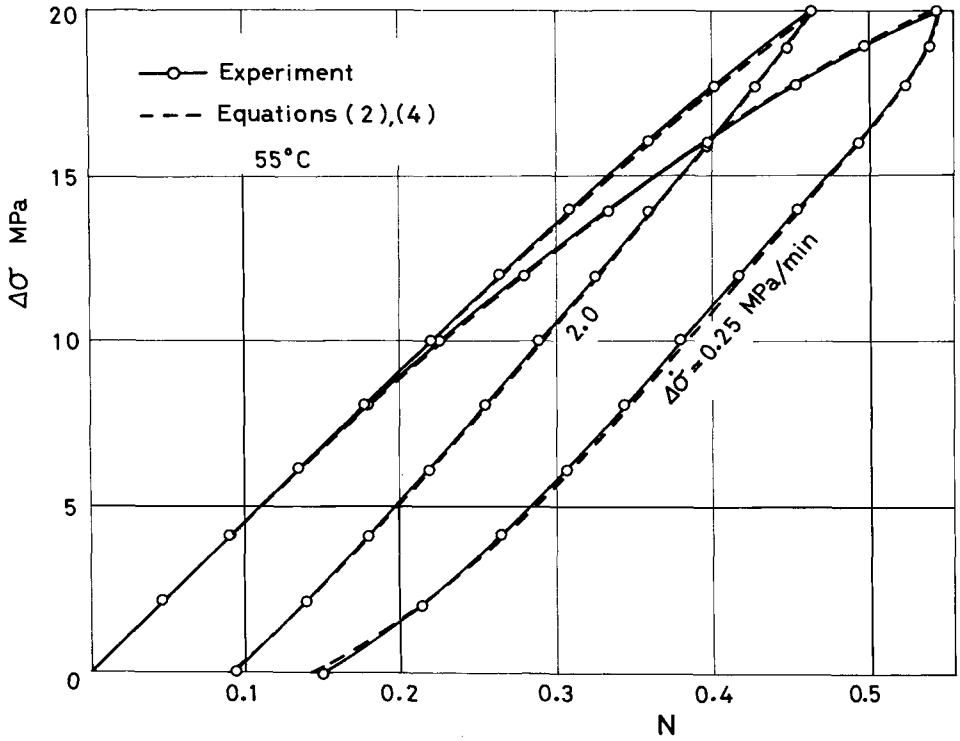

Fig. 3. Relations between $\Delta\sigma$ and the fringe order per unit thickness N corresponding to Figure 1.

As examples obtained for the variable stress rates, Figures 4 and 5 show the relations between $\Delta\sigma$ and ΔG for the conditions 1 and 4, respectively. In these figures, ΔG in the loading process is divided into the elastic part ΔG_e and the inelastic part ΔG_i by the broken line, and $\Delta\bar{G}$ in the unloading process is divided into the elastic part $\Delta\bar{G}_e$ and the inelastic part $\Delta\bar{G}_i$ by the broken line as shown in Figure 1. The broken line in the unloading process was decided from the preliminary tests for the cases of low unloading stress and of larger value of stress rate so as the inelastic part $\Delta\bar{G}_i$ may be neglected. Each symbol in Figures 4 and 5 is plotted using the average value of the three test results. The solid curves with symbols in Figures 6 and 7 show the experimental relations between $\Delta\sigma$ and the fringe order per unit thickness N corresponding to the experimental results shown in Figures 4 and 5, respectively.

DISCUSSIONS AND CONCLUDING REMARKS

The inelastic strain is strongly influenced by the stress rate for the cases (a) and (b) as shown in Figures 4 and 5. The isochromatic fringe order of the birefringence due to the inelastic strain is also strongly affected by the stress rate for the cases (a) and (b) as shown in Figures 6 and 7.

The broken curves in Figures 6 and 7 calculated from Eq. (2) using the optical constants C_1, C_2 obtained above and ΔG_i in Figures 4 and 5 for the loading process and from Eq. (4) using the optical constants $\bar{C}_1$, $\bar{C}_2$ obtained above and $\Delta\bar{G}_i$ in Figures 4 and 5 for the unloading process agree well with the corresponding experimental results represented by the solid curves with symbols, respectively, which were not used in determining the values of optical constants. The similar correspondences between the experimental results and the deduced birefringence relations were also obtained for the conditions 2 and 3 shown in Table I.

The deduced birefringence relations for the loading and unloading processes obtained from the cases of constant stress rate, neglecting the small amount of error, give fairly good agreement with the actual observations of the plastically deforming cellulose nitrate under several variable stress rates.

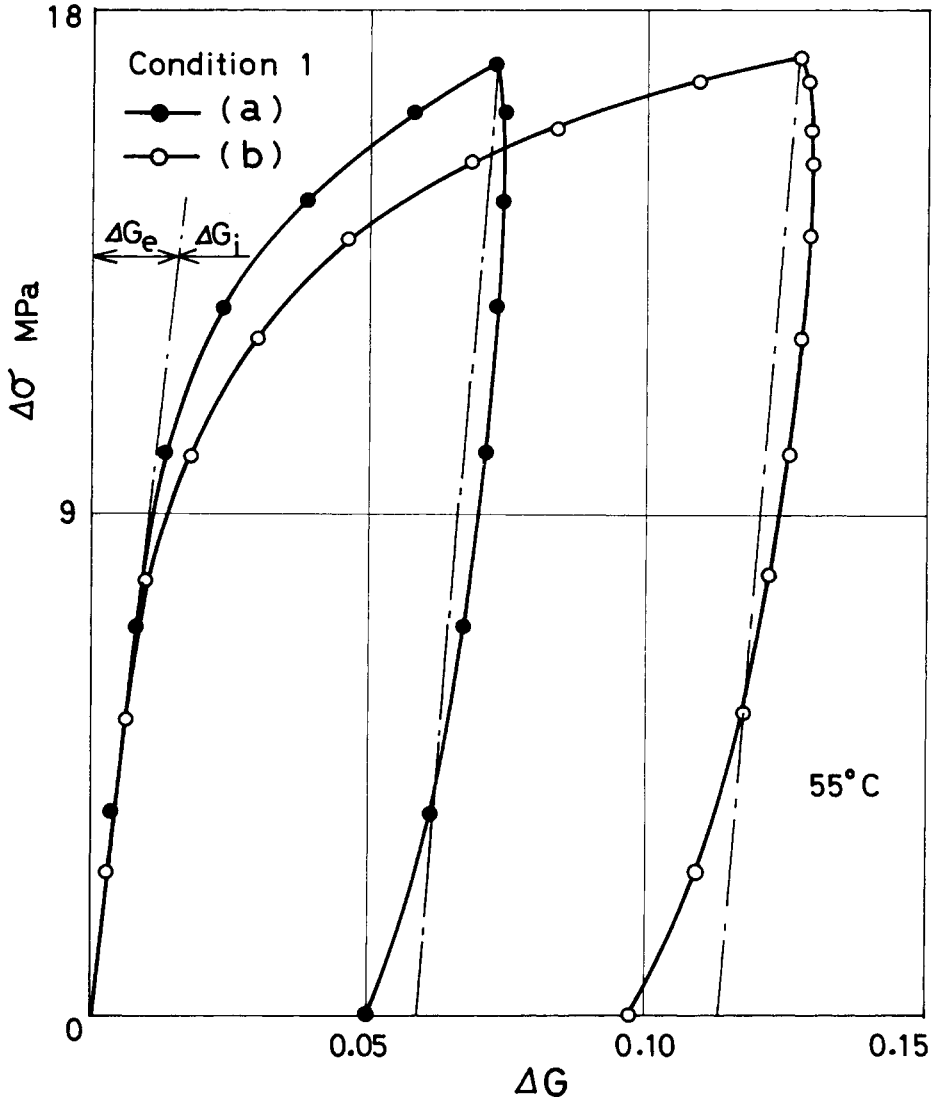

Fig. 4. Relations between $\Delta\sigma$ and ΔG for the conditions 1(a) and 1(b).

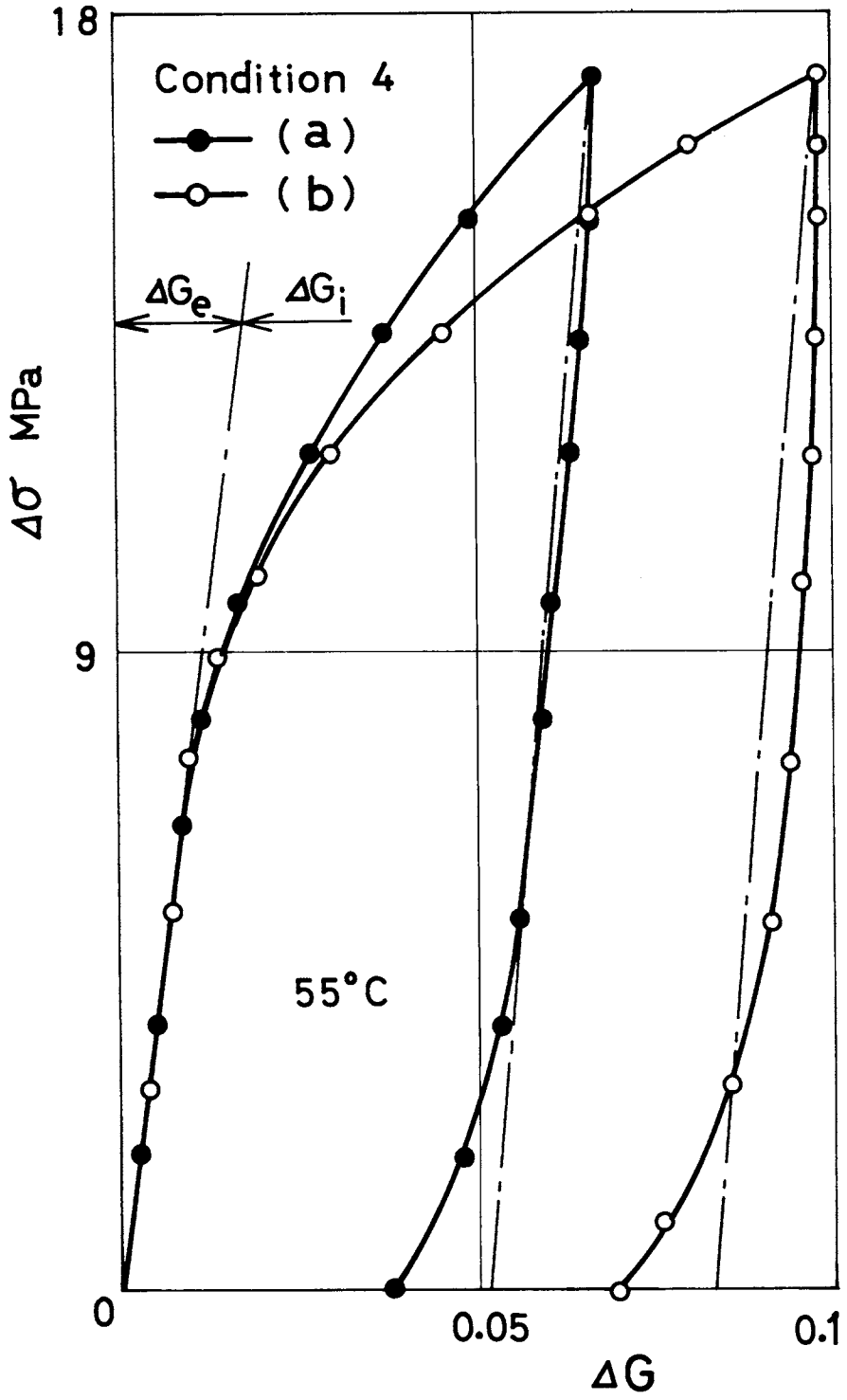

Fig. 5. Relations between $\Delta\sigma$ and ΔG for the conditions 4(a) and 4(b).

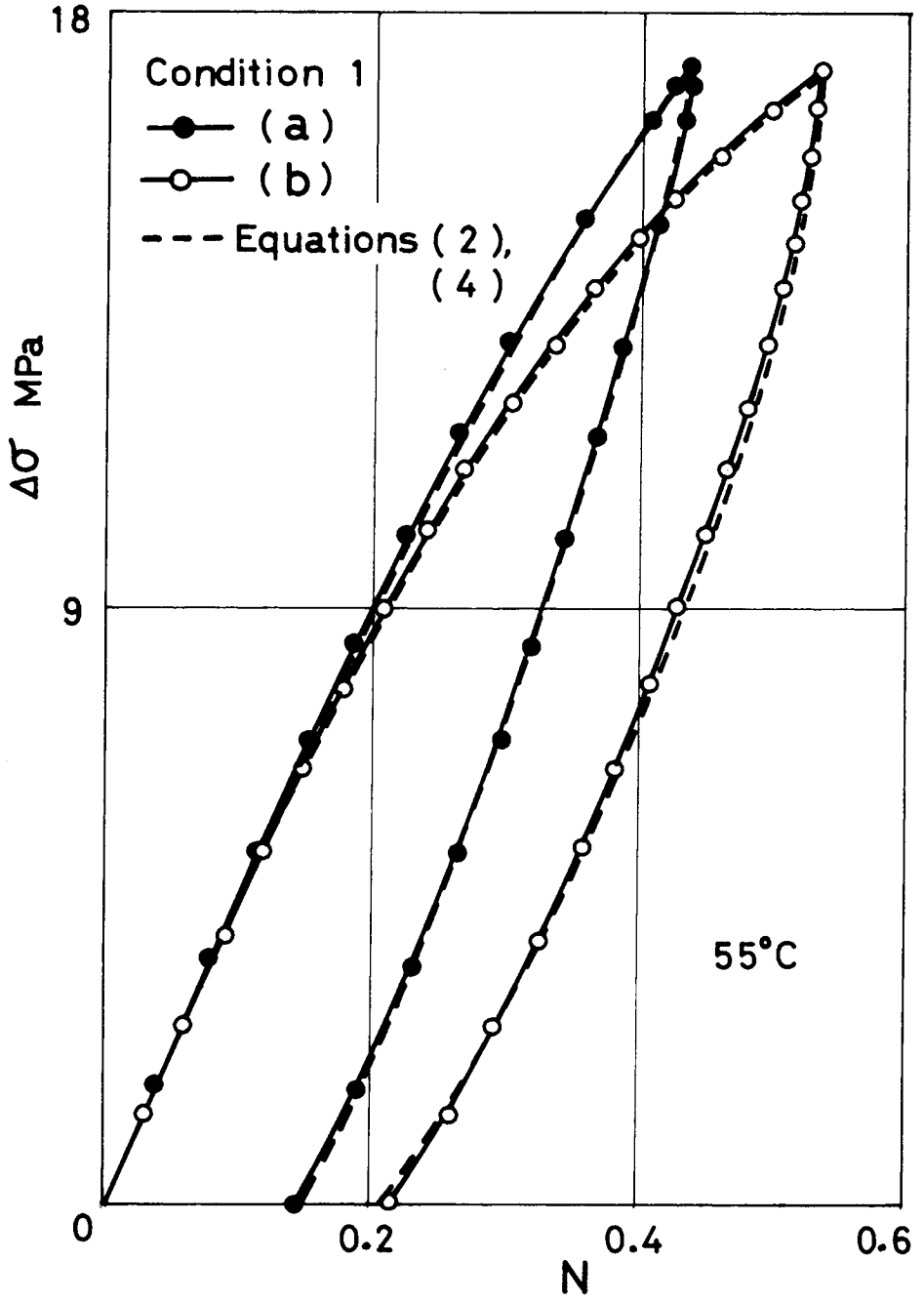

Fig. 6. Relations between $\Delta\sigma$ and the fringe order per unit thickness N for the conditions 1(a) and 1(b).

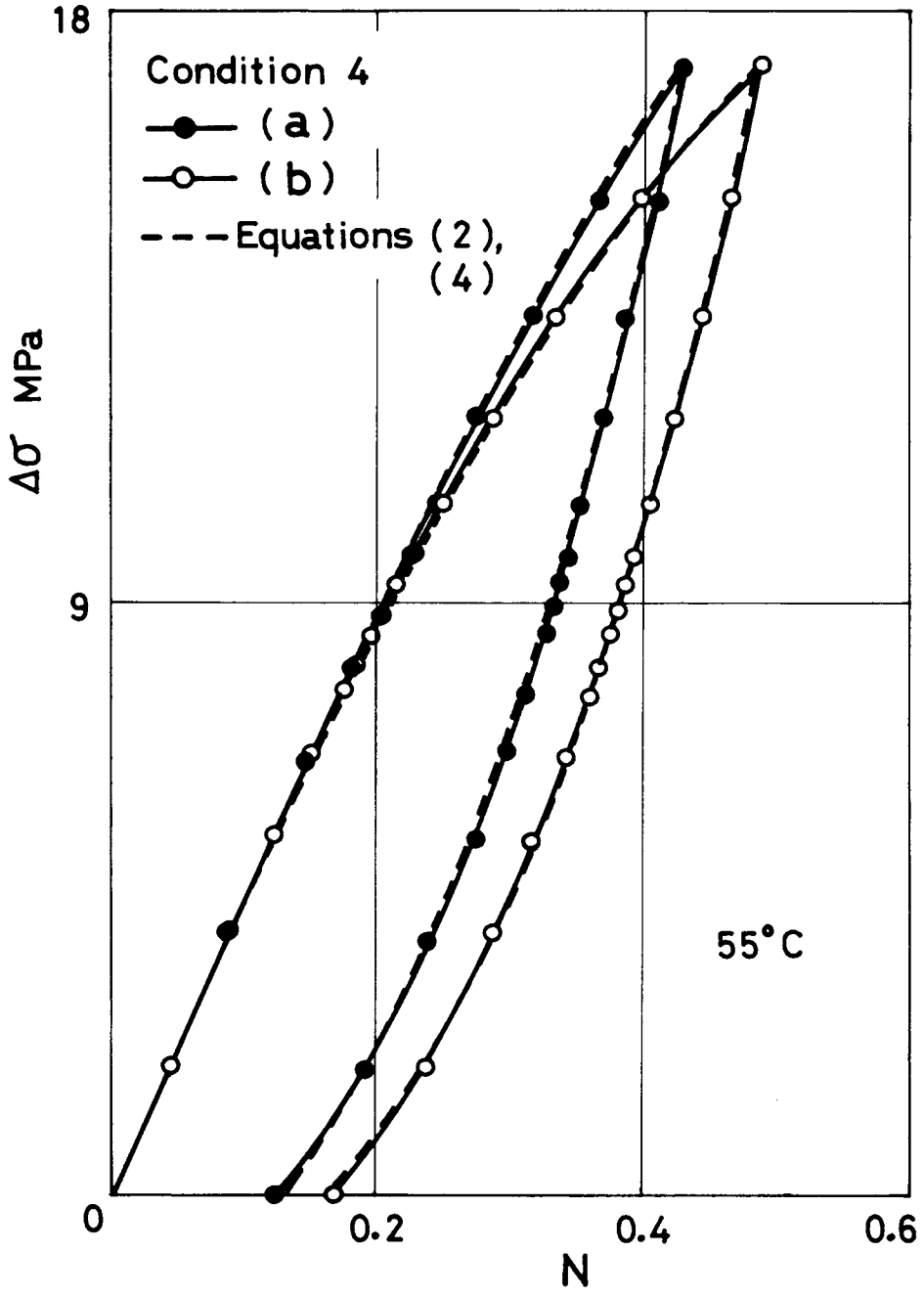

Fig. 7. Relations between $\Delta\sigma$ and the fringe order per unit thickness N for the conditions 4(a) and 4(b).

References

1. T. Nishitani and T. Ohnishi, *J. Appl. Polym. Sci.*, **25**, 1807 (1980).
2. T. Nishitani and N. Tekeuchi, *J. Appl. Polym. Sci.*, **28**, 1539 (1983).
3. Y. C. Fung, *Foundations of Solid Mechanics*, Prentice-Hall, Englewood Cliffs, N.J., 1965.
4. L. D. Landau and E. M. Lifschitz, *Electrodynamics of Continuous Media*, Pergamon, Oxford, 1960.
5. A. Sommerferd, *Optics*, Academic, New York, 1957.
6. D. C. Leigh, *Nonlinear Continuum Mechanics*, McGraw-Hill, New York, 1968.
7. Y. Ohashi, *Br. J. Appl. Phys.*, **16**, 985 (1965).
8. R. B. Heywood, *Photoelasticity for Designers*, Pergamon, Oxford, 1969.
9. J. W. Dally and W. F. Riley, *Experimental Stress Analysis*, McGraw-Hill, New York, 1965.

TADASHI NISHITANI
SHOJI YAMASHITA

Division of Applied Mechanics, Suzuka College of Technology
Suzuka, 510-02, Japan

Received December 20, 1985
Accepted January 13, 1986